New Strategies in Cancer Nanomedicine

Rong Tong[1,2] and Daniel S. Kohane[1]

[1]Laboratory for Biomaterials and Drug Delivery, Department of Anesthesiology, and Division of Critical Care Medicine, Boston Children's Hospital, Harvard Medical School, Boston, Massachusetts 02115; email: daniel.kohane@childrens.harvard.edu

[2]Koch Institute, Massachusetts Institute of Technology, Cambridge, Massachusetts 02139

Annu. Rev. Pharmacol. Toxicol. 2016. 56:41–57

First published online as a Review in Advance on October 28, 2015

The *Annual Review of Pharmacology and Toxicology* is online at pharmtox.annualreviews.org

This article's doi: 10.1146/annurev-pharmtox-010715-103456

Keywords

nanomedicine, nanoparticle, self-immolative polymer, stimulus-responsive drug delivery, triggered drug delivery, tumor penetration, PEGylation, circulation, tumor targeting, cancer immunology

Abstract

We review recent progress in cancer nanomedicine, including stimulus-responsive drug delivery systems and nanoparticles responding to light for phototherapy or tumor imaging. In addition, several new strategies to improve the circulation of nanoparticles in vivo, tumor penetration, and tumor targeting are discussed. The application of nanomedicine in cancer immunology, a relatively new type of cancer therapy, is also highlighted.

INTRODUCTION

Cancer nanomedicine refers to the application of nanotechnology-based therapeutics and imaging agents for the diagnosis, monitoring, prevention, and treatment of cancer (1). Cancer nanomedicine is expected to change chemotherapy by delivering a wide range of payloads with favorable pharmacokinetics, capitalizing on molecular targeting for enhanced specificity, efficacy, and therefore safety. Nanomaterial sizes below 100 nm match the length scales of the openings in the relatively leaky tumor vessel endothelium, and lymphatic dysfunction in tumor causes poor clearance of nanomaterials; both allow for enhanced permeation and retention (EPR) of nanoparticles (NPs) into tumors (2). The EPR effect has been demonstrated to be the key pharmacokinetic feature for passive tumor targeting and reduced systemic toxicity with cancer nanomedicines (3).

Many nanomaterials have been employed as delivery vehicles for drugs and/or imaging agents. They have included liposomes; polymer carriers, such as micelles, hydrogels, polymersomes, dendrimers, and nanofibers; metallic nanoparticles (e.g., gold, silver, titanium); carbon nanostructures (e.g., nanotubes, nanodiamonds, graphene); inorganic particles, such as silica particles; and hybrid nanomaterials (4). Different classes of nanomaterials with distinctive properties are optimal for specific applications. For example, the incorporation of chemotherapeutic agents in liposomal or polymeric NP delivery vehicles has resulted in improved drug solubility, reduced drug clearance, reduced drug resistance, and enhanced therapeutic effectiveness (5, 6). Several NP therapeutics [e.g., Doxil™ (approximately 100-nm PEGylated liposome loaded with doxorubicin) and Abraxane™ (approximately 130-nm albumin-bound paclitaxel NPs)] have been approved by the FDA and have shown improved pharmacokinetics and reduced adverse effects compared with their parent drugs (3). Other polymeric NPs that deliver small-molecule chemotherapeutics or small interference RNA (siRNA) have also entered clinical trials (7, 8). In addition, metallic particles are promising therapeutic agents that convert light to heat (the photothermal effect) to kill cancer cells, with clinical trials in head and neck cancer and lung cancers. Small-sized inorganic NPs (e.g., silica NPs) are in clinical trials as multimodal imaging agents for lesion detection and cancer staging (9).

This review provides an overview of recent progress toward in vivo application of cancer nanomedicine. We highlight some new nanomaterials in cancer nanomedicine, including new stimulus-responsive drug delivery systems and new cancer imaging NPs. We then discuss some emerging strategies to enhance the in vivo performance of nanomaterials by improving circulation, tumor penetration, and tumor targeting. Nanomaterials for cancer immunotherapy are also reviewed. Some of these new technologies or strategies may not be translated for clinical oncology in the immediate future, but they are of great research interest and are potentially relevant to the treatment of other diseases.

STIMULUS-RESPONSIVE DRUG DELIVERY

In recent years, there have been increasing efforts to develop stimulus-responsive nanomaterials that utilize endogenous or exogenous stimuli to facilitate drug delivery (10, 11), usually by enhancing the preferential accumulation of those nanomaterials in target tissues. Endogenous stimuli include small molecules, proteins (enzymes), nucleic acids, peptides, electron transfer reactions, viscosity, osmotic pressure, and local environmental factors, such as pH, temperature, or redox state. One of the problems in designing materials that respond to an endogenous stimulus is that some environmental triggers (e.g., pH or a redox trigger) are found to varying degrees in multiple locations throughout healthy or diseased tissue, which could activate nanomaterials at unwanted

times or in unwanted locations. Exogenous stimuli, such as ultrasound, electromagnetism, light, and temperature, can be applied directly to a tissue of interest to drive localization or release of cargo (12, 13). Such spatiotemporal control over the activation of materials may maximize cargo release at the desired site, and thus minimize side effects in surrounding, healthy tissue. Some means of activation such as ultrasonic waves, sophisticated light sources, or strong magnetic fields may not always be practical or cost-effective. Another problem related to the application of exogenous stimuli is the depth of tissue penetration that can be expected. A major challenge with many stimulus-responsive delivery approaches is to translate relatively complicated designs from the bench to a successful in vivo application. Triggerable systems have been reviewed elsewhere (10–13); here, we highlight progress in this area. New nanomaterials for stimulus-responsive drug delivery include self-immolative polymers, which degrade upon stimulation; nanomaterials with autonomous motion; and nanomaterials that respond to near-infrared (NIR) light (for triggered drug delivery and tumor imaging).

Self-Immolative Polymer Degrades Upon Stimulation

Self-immolative polymers, which degrade in response to various stimuli, have been designed for triggered drug delivery (14). The backbone of such polymers is stable until a stimulus-responsive trigger group is removed. The functional group exposed in this process subsequently initiates a cascade of reactions that lead to complete depolymerization. The stimulus-responsive trigger group has been designed to be sensitive to light, pH, oxidative stress, reductive condition, or enzymes (14–17). One such polymer backbone is a polycarbamate based on 4-aminobenzyl alcohol derivatives, which degrades entirely through intramolecular 1,6-elimination reactions via quinone-methide intermediates (**Figure 1*a***) (16, 18). Polycarbamates that depolymerize by alternating elimination and cyclization reactions have also been synthesized (**Figure 1*b***) (19). Polyglyoxylate is another new class of self-immolative polymer, with monomers that can be directly prepared from fumaric or maleic acid (**Figure 1*c***); the monomers of the other two self-immolative polymers require multistep syntheses (20). A NIR-light sensitive NP based on quinone-methide polymers was developed for triggered drug delivery (21); upon irradiation with light, the self-immolative polymer backbone decomposed and the encapsulated drug was released.

Nanomaterials with Autonomous Motion

Some nanomaterials are capable of propelling themselves, with or without an externally applied stimulus. It is hypothesized that this approach could be used to control nanomaterial localization or tissue penetration. The first reported nanomaterial with autonomous motion involved the asymmetric positioning of a platinum-based catalyst at one end of a gold-platinum nanorod (22). The platinum catalyst converted hydrogen peroxide to oxygen, creating an oxygen concentration gradient that created interfacial tension (on the order of piconewtons) to propel the nanorod. External stimuli such as acoustic waves (23, 24) or magnetism (25–27) have also been used to direct nanomaterial motion. For example, perfluorocarbon emulsions (approximately 300 nm) were loaded inside hollow gold microtubes. An ultrasound pulse triggered vaporization of the perfluorocarbon emulsions, which propelled the nanorod (23). In another example, flexible Au/Ag/Ni nanowires, with a gold head, a nickel tail, and a partially dissolved and weakened silver bridge, responded to external rotating magnetic fields with cyclic mechanical deformations at the flexible silver linker

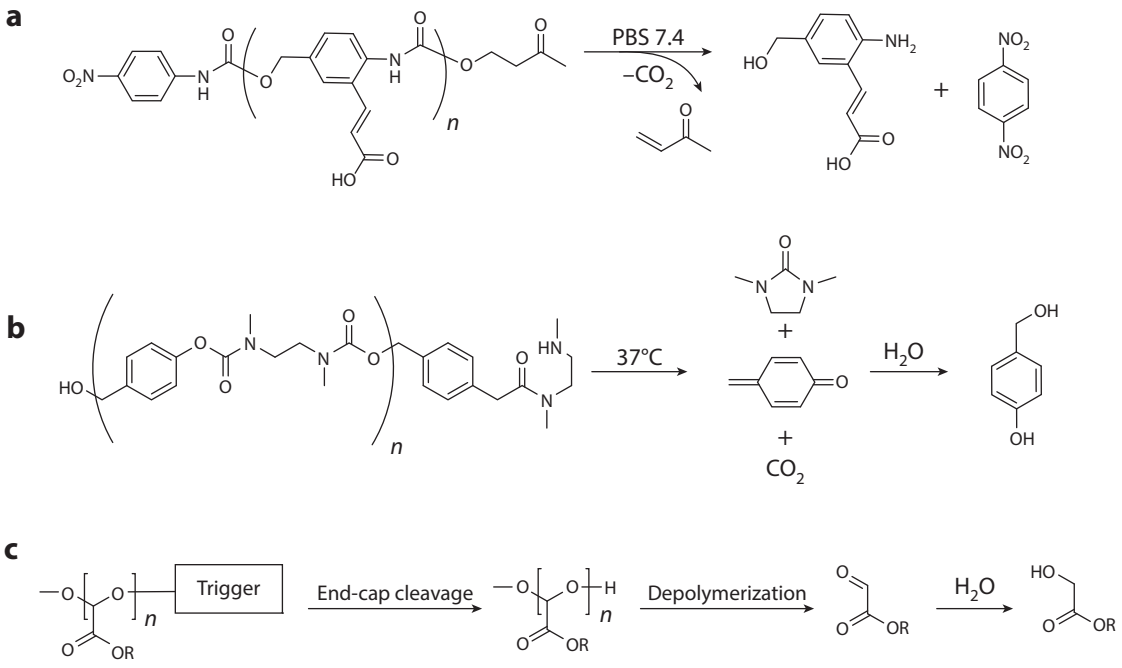

Figure 1

Self-immolative polymers degrade upon triggering. (*a*) A polycarbamate depolymerizes via a quinone-methide intermediate. (*b*) A different polycarbamate depolymerizes via alternating cyclization and elimination. (*c*) Polyglyoxylate self-depolymerizes to glyoxylic acid.

(27). Such nanomaterials have been investigated to enhance cell uptake or tissue penetration in vitro (26). Their practicality in directing motion in vivo remains to be demonstrated.

The Use of Near-Infrared Light to Access Deep Tissue

Light is a useful stimulus for triggered drug delivery and imaging. However, light propagation in tissue is affected by scattering owing to tissue heterogeneity and by absorbance by water and endogenous dyes such as hemoglobin (28). The maximum skin permeability to light occurs in the ranges circa 650–900 nm [the so-called NIR light window I (NIR-I)] (29, 30) and 1,100–1,400 nm [NIR window II (NIR-II)] (**Figure 2*a***) (31). NIR light can propagate through tissues with less attenuation than can shorter-wavelength light (28, 32). The use of NIR light therefore has significant advantages for phototherapy and optical imaging within deep tissues. Consequently, many NIR-I wavelength fluorescent dyes and inorganic NPs (e.g., gold NPs) have been applied as contrast agents for tumors in preclinical animal models or human patients (33, 34). Nonetheless, the tissue penetration depth for noninvasive imaging using these agents is limited (35). NIR-II may be more advantageous for in vivo imaging than NIR-I because of its reduced photon absorption and scattering by tissues, its negligible tissue autofluorescence, and its deeper tissue penetration (36, 37). Currently, only a few nanomaterials (e.g., single-walled carbon nanotube, quantum dots) (31, 36–38) have been studied in preclinical animal models using light in the NIR-II window. The frequency-domain photon migration technique, which is a sophisticated technique that eliminates background light, may extend the depth to which light in the NIR window can be used for imaging up to 10 cm, which is more practical for clinical use (39, 40).

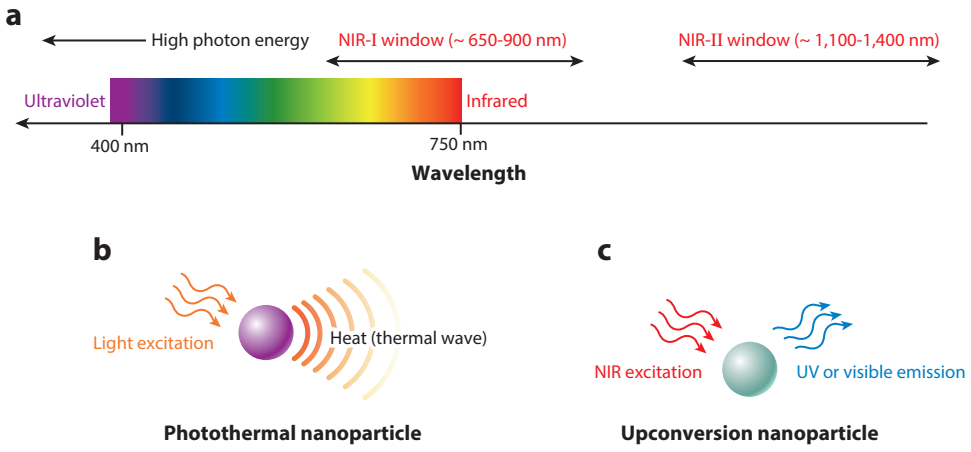

Figure 2

Light for in vivo imaging and therapy, and light-triggered nanoparticles (NPs). (*a*) The electromagnetic spectrum of ultraviolet (UV), visible, and infrared (IR) light and of the near-infrared (NIR)-I and NIR-II window for in vivo imaging and phototherapy. (*b*) Schematic illustration of a metallic NP that can absorb visible or NIR light and dissipate such absorbed light energy as heat (photothermal effect). (*c*) Schematic illustration of upconversion NPs that can be excited by NIR light to emit UV or visible light.

Nanomaterials for Light-Triggered Drug Delivery

Local heating of tumors to about 41–43°C, known as hyperthermia therapy, has been shown to increase the blood flow to and permeability of tumor vessels (41). Liposomes have been designed to release drugs when tumors are preheated (42), and such liposomes containing doxorubicin are currently in clinical trials (43). However, such conventional hyperthermia often takes approximately 30–60 min to heat tumors. More rapid heating (within minutes) (44) can be achieved by irradiating metallic NPs that have surface plasmon resonance (e.g., gold NPs and CuS NPs), which efficiently absorb light and convert it to heat (**Figure 2*b***) (45, 46). The photothermal properties of gold NPs have been utilized to enhance the accumulation of subsequently administered conventional NPs in tumors (47). In one application, the photothermal properties of gold NPs disrupted tumor vessels; the resulting local overexpression of fibrin (44) was used as a target for the accumulation of a second group of NPs that were surface modified with a peptide targeting fibrin, administered 72 h later (47, 48). Organic NPs can be used in a similar manner. Nanoliposomes composed of lipid conjugates of the photosensitizer pyropheophorbide (a chlorin analogue) can efficiently absorb and transfer light energy into heat for photothermal therapy. The same nanoliposome can also carry doxorubicin for chemotherapy. Irradiation of the nanoliposomes in tumors induces photothermal effects, and the generated heat enhances tumor permeation, which allows for doxorubicin accumulation over 24 h (49, 50).

The type of NPs used in photothermal therapy can be also used as the heat source for thermoresponsive drug delivery systems. For instance, thermoresponsive polymers coated on hollow porous gold nanostructures (51) shrink upon irradiation, uncovering the pores and allowing drug efflux. The use of light to trigger drug release from NPs has been reviewed (12).

Light-triggered nanomaterials have also been used to enhance tumor penetration and drug delivery. We recently developed a photoswitchable spiropyran-based drug delivery NP with a light-induced reversible volume change from 100 to 40 nm (52). The volume change of the

monodisperse NPs enabled repeated drug release, and enhanced NP diffusion into tumors. Triggered release of docetaxel from the NPs decompressed tumor vessels by inducing tumor cell apoptosis, and prompted NP penetration into and accumulation in the tumor interior (53).

Nanomaterials Using Near-Infrared Light for Tumor Imaging

Conventional approaches to making nanoparticulate tumor imaging agents include loading contrast agents inside NPs or onto their surfaces. Alternatively, the NPs themselves can be imaging agents. In particular, a class of new imaging nanomaterials that can be activated with NIR lasers has been developed recently: upconversion NPs. Most fluorophores emit light at a longer wavelength (lower energy) than their excitation wavelength (so-called downconverting photoluminescence or Stokes emission). In contrast, upconversion NPs can be excited with continuous-wave (power is constant over time, in contrast to pulsed lasers) NIR light (900–1,000 nm) to emit at shorter wavelengths such as visible and UV light (**Figure 2*c***) (54–57). Upconversion NPs are usually $NaYF_4$ NPs doped with trivalent rare-earth ions (e.g., Yb^{3+}, Tm^{3+}, Er^{3+}, Ho^{3+}) that absorb 980-nm light. Such upconversion NPs have attracted considerable attention in bioimaging applications because of their large anti-Stokes shifts (>400 nm), sharp emission bandwidths, high resistance to photobleaching, stable emission, ability to be detected deep within tissue (using NIR light), and ability to undergo surface modification with biomolecules (58). However, tissue overheating (and associated phototoxicity) can occur when using upconversion NPs because 980-nm light is strongly absorbed by water. Such light-induced injury can be minimized by reducing the absorption wavelength from 980 to 800 nm using core-shell $NaGdF_4$ upconversion NPs codoped with Nd^{3+}, Yb^{3+}, and Er^{3+} (59, 60). An alternative method involves using NIR-absorbing organic dyes (e.g., cyanine) coordinated on the surface of upconversion NPs. The dye absorbs NIR light (650–850 nm) and then transfers the energy to Yb^{3+} (absorption at 900–1,000 nm); the energy is then extracted by Er^{3+} inside the upconversion NPs, emitting visible light (61). The toxicity and safety of such lanthanide-doped upconversion NPs for in vivo applications is still being evaluated. Recently, organic upconversion NPs have been prepared for bioimaging (62): Albumin-dextran NPs contained photosensitizers that could absorb long-wavelength light and emitted short-wavelength light via triplet-triplet annihilation (two long-lived triplet state photons upconverting to a high-energy singlet state for emission). Such organic upconversion NPs have higher quantum efficiency than $NaYF_4$ upconversion NPs do for small-animal imaging (62).

NIR light can also be used for photoacoustic (optoacoustic) imaging. Photoacoustic imaging is an ultrasonic imaging technique in which wide-band ultrasonic waves can be induced by a pulsatile excitation laser (NIR laser) owing to thermoelastic expansion of tissues. The loss of signal in photoacoustic imaging is negligible compared with other optical imaging techniques because acoustic waves have two to three orders of magnitude less scattering in tissue than light (63). Inorganic NPs (e.g., carbon nanotubes and gold NPs; 64–68) have recently been shown to be improved contrast agents for photoacoustic imaging, with better photophysical properties and longer circulation times than small-molecule agents. The combination of photoacoustic tomography imaging techniques with the potential therapeutic effects from metallic NPs (e.g., photothermal therapy) may provide a strategy for simultaneous diagnosis and treatment of cancers (46). For example, tumors with accumulated hollow gold NPs could be imaged using photoacoustic technology (66). Accurate and efficient ablation of a tumor by photothermal therapy has been achieved by simply switching laser power from a power suitable for photoacoustic imaging (50 mW/cm^2) to one suitable for photothermal therapy (16 W/cm^2, 3 min) (66).

STRATEGIES FOR PROLONGING NANOPARTICLE CIRCULATION

NPs have prolonged circulation in the blood compared with small-molecule drugs (<5 nm) (5, 69). Macrophages in the reticuloendothelial system can engulf and clear injected NPs, which can lower the dose of NPs reaching tumors. Moreover, macrophage uptake of NPs can lead to compromised host defenses (owing to the saturation of macrophage uptake capability by NPs) (70), release of toxic by-products (from exposing NPs to a highly oxidative environment upon phagocytosis) (71), and redistribution of NPs to the liver and spleen that can induce delayed or chronic toxicity (72–74). Coating NPs with poly(ethylene glycol) (PEG), which is known as PEGylation and mimics a cell's glococalyx (75–77), can suppress protein absorption to NPs and delay the rate of NP uptake and clearance, greatly prolonging circulation time. However, PEGylation cannot eliminate macrophage uptake that is not mediated by serum absorption (78).

Another strategy for prolonging the circulation time is to change the aspect ratio of nanomaterials, which affects their interaction with cells (e.g., uptake) and with the hydrodynamic forces of flowing blood (79). For example, cylindrical micelles had much longer circulation times in vivo than their spherical counterparts (79). An intriguing approach to evading phagocytosis of NPs was to graft a synthetic small peptide that was computationally designed from CD47—a cell-surface marker of self that impedes macrophage uptake (80)—to mimic the CD47-CD172a interaction that inhibits phagocytosis. This peptide prolonged the circulation time of NPs in vivo (81).

OVERCOMING PHYSIOLOGICAL BARRIERS THAT PREVENT DEEP TUMOR PENETRATION

Nanoparticles with sub–100-nm sizes are optimal for the EPR effect (82). However, the transport of NPs or drugs into tumors from the bloodstream is impeded by tumor blood-flow stasis or collapsed tumor blood vessels (**Figure 3**) (3). NP access deep into tumors is hindered by the large distance between blood vessels in tumors and by the dense interstitial matrix—a complex assembly of collagen, glycosaminoglycans, and proteoglycans (83). For example, Doxil and Abraxane (both about 100 nm) are found trapped less than 100 μm away from vessels (84–87). In many tumors that are termed desmoplastic, blood vessels are surrounded by a dense stroma of matrix and noncancer cells (e.g., fibroblasts) (88). NPs must penetrate up to hundreds of micrometers through stroma to reach their target cancer cells. Deep penetration of NPs in tumors is necessary for therapeutic effect (89). Various physicochemical parameters of NPs have been studied to develop an understanding of NP-tumor interaction that might lead to enhanced tumor penetration. NP size is one crucial determinant of accumulation and penetration into tumor tissue. It is reported that approximately 30-nm polymeric micelles showed enhanced tissue penetration and potent antitumor activity in pancreatic tumors compared with larger NPs (90). In another example, 50-nm silica NPs showed deeper tissue penetration and higher accumulation in breast tumors over time, compared with 20 nm or larger NPs (91). Of note, recent studies showed that approximately 15-nm gold NPs surface decorated with siRNA could pass through a compromised blood-brain barrier and accumulate in glioblastoma (92). NP size appears to be a critical determinant of penetration into and accumulation within tumor tissue, although the effects of specific sizes depend on the particular formulation studied.

Antiangiogenic Therapy for Drug Delivery

Antiangiogenic therapy can normalize the tumor vasculature by inducing vessel maturation such that there is increased perfusion and more evenly distributed vasculature within tumors (93). This

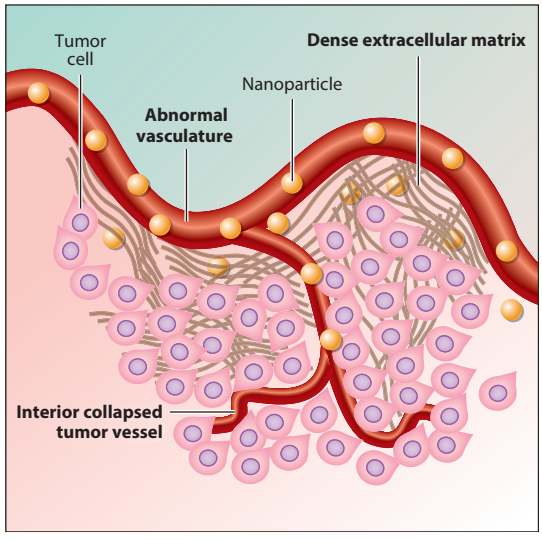

Figure 3

Scheme of the delivery barriers that prevent deep penetration of nanoparticles (NPs) in tumors. The abnormal tumor vasculature, dense collagen matrix, and collapsed vessels in the tumor interior present barriers to NP penetration deep into tumors.

normalization has been suggested as a means of modulating and perhaps improving NP delivery into tumors. Recently it was found that blocking vascular endothelial growth factor receptor-2 (VEGFR2) in mouse mammary tumors greatly improved the delivery of small NPs (12 nm) but not large NPs (125 nm) (94). The explanation for this observation may be that the maturation of the tumor vasculature by the anti-VEGFR2 agent decreased the tumor vessel pore size, which then allowed only the smaller NPs (<60 nm) to be rapidly transported in tumor tissue.

Targeting Tumor Extracellular Matrix to Improve Drug Delivery

In solid tumors, penetration of macromolecular agents and NPs is affected by tumor stromal barriers such as the extracellular matrix (ECM) (e.g., collagen network) (85). Numerous studies have shown that ECM-degrading enzymes, such as collagenase or hyaluronidase, can improve NP penetration into solid tumors (84, 95, 96). However ECM-degrading agents may increase the incidence of metastasis (97). The antihypertensive drug losartan was recently found to reduce tumor collagen content by blocking angiotensin-II-receptor 1 and has been successfully used to enhance diffusive transport and efficacy of intravenously administered NPs such as Doxil (98, 99). However, in a recent multicenter Phase II clinical study, combined chemotherapy with gemcitabine and candesartan, a losartan analogue, failed to demonstrate prolonged progression-free survival in advanced pancreatic cancer patients (100). A safety concern was also raised because hypotension induced by candesartan was observed in some patients.

Tumor-Penetrating Peptides for Enhanced Tumor Penetration

Tumor-penetrating peptides, such as iRGD (a cyclic RGD peptide, CRGDKGPDC) and Lyp-1 (CGNKRTRGC), were identified by phage library screening and were able to enhance drug or NP penetration into tumors (101, 102). The iRGD peptide is proteolytically degraded into

its active form and bound to neurophilin-1, which is expressed in tumor vasculature and tumor cells, and it induces endocytic bulk transport through tumor tissue; the detailed pathway for tissue penetration and endocytosis is still being elucidated (103). Co-administration of such peptides with Abraxane NPs significantly increased their intratumoral accumulation (101).

BIOORTHOGONAL CHEMISTRY FOR TUMOR TARGETING

Selective targeted delivery of drugs to tumors is a major challenge in cancer therapy. Conjugation of tumor-targeting ligands to NPs has been widely used for tumor-selective drug delivery or diagnostics. Recently, the use of bioorthogonal chemistry for tumor targeting has emerged as a new strategy that can be independent of the use of targeting ligands. Bioorthogonal chemistry refers to a variety of chemical reactions using functional groups that generally do not occur in the host creature and that do not interfere with native biochemical reactions (104). Such reactions include azide-alkyne cycloaddition, azide-phosphine Staudinger ligation, and tetrazine-cyclooctene Diels-Alder reactions (105, 106) (**Figure 4*a***). Bioorthogonal chemistry can be used for cell surface

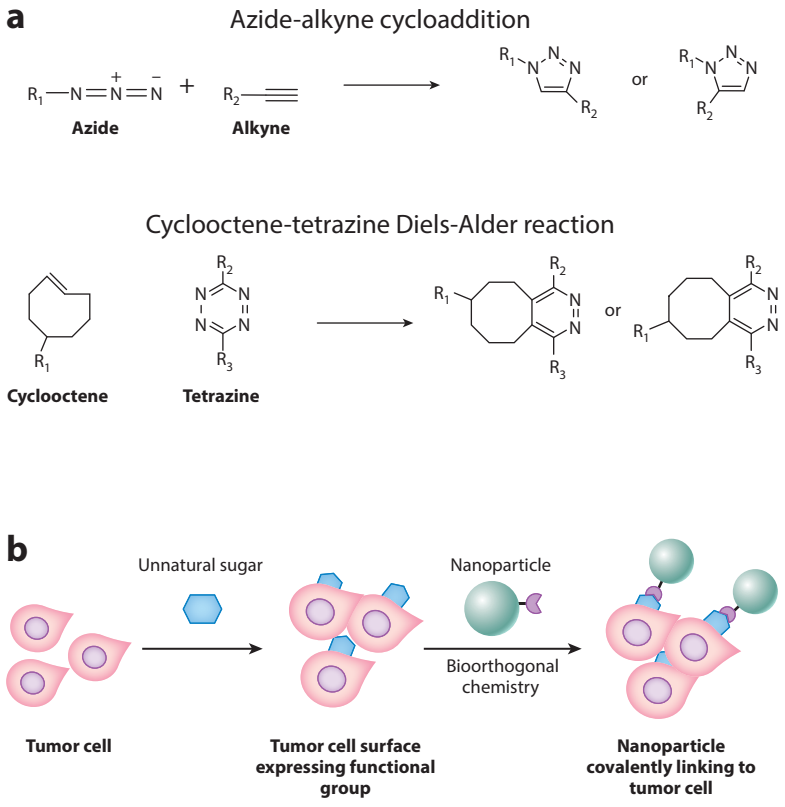

Figure 4

Bioorthogonal reactions for tumor targeting. (*a*) Examples of bioorthogonal reactions: azide-alkyne cycloaddition and cyclooctene-tetrazine Diels-Alder reaction. (*b*) Schematic illustration of tumor targeting using bioorthogonal reactions. Tumor cells are first fed with unnatural aminosugars that contain one functional group for the bioorthogonal reaction. That functional group is later expressed on the tumor cell surface and can react via a bioorthogonal reaction with nanoparticles that are surface modified with another functional group.

modification in vitro. For example, aminosugars containing one unnatural functional group can be taken up by cells and expressed on their surfaces; the introduced functional group can undergo bioorthogonal chemistry to artificially label the cells (107). Such in vitro cellular modification inspired a two-step in vivo tumor-targeting strategy to enhance intratumoral NP accumulation (108). The first step involved treating the tumor, by intratumoral injection, with an unnatural glycan containing an azide group. Cancer cells would take up glycans and express them, with azide groups, on cell surfaces. When NPs containing alkyne groups were administered systemically, they underwent a bioorthogonal reaction with the azides in the tumor, which led to enhanced intratumoral accumulation of NPs (**Figure 4*b***). Bioorthogonal tumor-targeting strategies can also be applied to tumor imaging. Tumor cells prelabeled with antibodies modified with cyclooctene were implanted subcutaneously, and perfluorocarbon microbubbles surface modified with tetrazine groups were injected systemically and reacted with the cyclooctene on the tumor cells, which could then be better imaged by ultrasound in vivo (109). In another example of tumor imaging using bioorthogonal chemistry, mice were first injected intravenously with a tumor-targeting peptide modified with a tetrazine group. Liposomes containing the short-lived positron emission tomography (PET) tracer ^{18}F were surface modified with cyclooctene and administered systemically. The liposome with cyclooctene quickly reacted with tetrazine-modified peptides bound to tumor cells, which highlighted the tumor for PET imaging. The prolonged circulation of liposomes allowed for imaging with enhanced signal intensity (110). An alternative targeting strategy that takes advantage of biotin-streptavidin binding has also been reported: Biotin-coated gold NPs were first injected into tumor-bearing mice and accumulated in the tumors via EPR. A streptavidin-labeled contrast agent was then administered to image the tumor (111). Bioorthogonal approaches are intriguing, but the initial step of introducing the unnatural functional group into tumors or tissues can be technically challenging.

NANOMATERIALS FOR CANCER IMMUNOTHERAPY

Immunotherapy has become a promising approach for cancer treatment and management, owing to the recent success of proof-of-concept clinical trials (112). Current cancer immunotherapeutics target cancer cells by generating host immune cell responses to tumor antigens.

The use of nanomaterials in cancer immunotherapy can deliver agents to specific organs (e.g., lymph nodes) or cells. In particular, NPs have been used to target immune cells inside lymph nodes (LNs) or mucosal tissues to induce immune responses toward tumors. NP size directly affects which immune cells the NPs enter. Upon footpad injection in mice, particles between 500 and 2,000 nm are generally processed by antigen-presenting cells (APCs) at the injection site, whereas sub–200-nm NPs can traffic to the LNs, where they are captured by LN-resident dendritic cells (DCs) (113). After intradermal injection, 25-nm NPs can flow through lymphatic capillaries to the draining LNs, whereas 100-nm NPs cannot be transported to LNs (114). Such size-dependent LN-targeting has been used for both imaging and vaccination. In one example, 16-nm iron oxide/zinc oxide NPs carrying carcinoembryonic antigen were injected into the mouse footpad and trafficked to draining LNs. The NPs could be imaged by MRI because of the iron oxide, and they were also effective as vaccines, showing strong cytotoxic T lymphocyte responses and significant reduction of tumor growth (115). NPs have been designed to target LNs for vaccination against tumors. The immune-modulator molecule CpG and an adjuvant (ovalbumin) were conjugated onto the surfaces of separate 30-nm polymeric NPs and were injected intradermally. Both NP conjugates rapidly drained to the LNs and enhanced the DC uptake of both antigen and adjuvant (116). This codelivery strategy induced potent effector $CD8^+$ T cells and a more

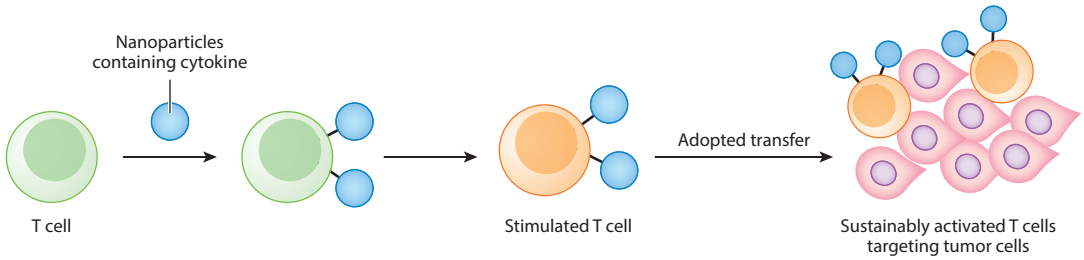

Figure 5

Scheme of nanoparticle (NP)-tethering T cells for adoptive cancer immunotherapy. T cells are linked with NPs that contain cytokines, which can stimulate the T cells to kill tumor cells. The activated T cells are adoptively transferred in vivo; NPs release cytokines locally to sustainably stimulate T cells to target tumors.

efficacious memory recall by cytotoxic T cells upon reinjection of tumor cells, compared with the response when NP-conjugated antigen was used with free adjuvant.

NPs can be delivered via pulmonary administration to the numerous APCs in the lung, which can take them up avidly (117). A subset of such lung APCs can further transport NPs containing antigens to DCs in draining LNs. In mice vaccinated by pulmonary administration of nanovesicles loaded with antigen and Toll-like receptor agonist, which both promote cytotoxic T cell response (118), the antigen was detected in LNs for at least 7 days, whereas pulmonary immunization with soluble vaccines led to rapid antigen clearance. Strong T cell responses elicited by this pulmonary vaccine nanovesicle enhanced protective immune responses in tumors.

Cell therapy for cancer immunotherapy (e.g., adoptive transfer of T lymphocytes) represents another promising approach (119). In this approach, immune cells (e.g., T cells) are harvested and stimulated ex vivo with cytokines before they are reintroduced into the body. Cytokines used in such therapy may cause systemic toxicity, but they have to be kept at high concentrations near the administered therapeutic cells to maintain cell stimulation over an extended period. A new approach to overcome this problem is to directly tether cytokine-loaded NPs to the surfaces of the therapeutic cells prior to infusion (120). Liposomal NPs containing IL-15Sa and IL-21 were conjugated to thiol groups on the surfaces of T lymphocytes. The NP-tethering strategy greatly enhanced T cell survival and expansion after infusion and slowed tumor growth (**Figure 5**).

PERSPECTIVE

Cancer nanomedicine is a very rapidly growing field of translational medicine (121). Effective therapeutics and diagnostics for cancer require delivery to tumors with appropriate temporal resolution to achieve the most favorable pharmacokinetics. Various forms of tumor targeting, including stimulus-responsive drug delivery systems, can address this need. The development of new nanomaterials will be a crucial driver of progress in this field. However, a better understanding of the fundamental processes involved is necessary to overcome major hurdles in cancer nanomedicine, including NP circulation, biodistribution, tumor targeting, and tumor penetration. Further knowledge of cancer biology and oncology will enhance the rational design of NPs for specific cancers. Research is needed to develop new strategies to treat metastatic tumors, which account for the majority of cancer deaths (122). The early detection of tumor by NPs will also be useful for catching cancer at an early stage. Biocompatibility, toxicity, and the numerous formulation issues that pertain to all nanomaterials will remain important for the success of new cancer nanomaterials (123).

DISCLOSURE STATEMENT

The authors are not aware of any affiliations, memberships, funding, or financial holdings that might be perceived as affecting the objectivity of this review.

LITERATURE CITED

1. Moghimi SM, Hunter AC, Murray JC. 2005. Nanomedicine: current status and future prospects. *FASEB J.* 19:311–30
2. Matsumura Y, Maeda H. 1986. A new concept for macromolecular therapeutics in cancer-chemotherapy—mechanism of tumoritropic accumulation of proteins and the antitumor agent SMANCS. *Cancer Res.* 46:6387–92
3. Jain RK, Stylianopoulos T. 2010. Delivering nanomedicine to solid tumors. *Nat. Rev. Clin. Oncol.* 7:653–64
4. Chow EK-H, Ho D. 2013. Cancer nanomedicine: from drug delivery to imaging. *Sci. Transl. Med.* 5:216rv4
5. Gref R, Minamitake Y, Peracchia MT, Trubetskoy V, Torchilin V, Langer R. 1994. Biodegradable long-circulating polymeric nanospheres. *Science* 263:1600–3
6. Langer R. 1998. Drug delivery and targeting. *Nature* 392:5–10
7. Davis ME, Zuckerman JE, Choi CHJ, Seligson D, Tolcher A, et al. 2010. Evidence of RNAi in humans from systemically administered siRNA via targeted nanoparticles. *Nature* 464:1067–70
8. Hrkach J, Von Hoff D, Ali MM, Andrianova E, Auer J, et al. 2012. Preclinical development and clinical translation of a PSMA-targeted docetaxel nanoparticle with a differentiated pharmacological profile. *Sci. Transl. Med.* 4:128ra39
9. Phillips E, Penate-Medina O, Zanzonico PB, Carvajal RD, Mohan P, et al. 2014. Clinical translation of an ultrasmall inorganic optical-PET imaging nanoparticle probe. *Sci. Transl. Med.* 6:260ra149
10. Blum AP, Kammeyer JK, Rush AM, Callmann CE, Hahn ME, Gianneschi NC. 2015. Stimuli-responsive nanomaterials for biomedical applications. *J. Am. Chem. Soc.* 137:2140–54
11. Tong R, Tang L, Ma L, Tu C, Baumgartner R, Cheng J. 2014. Smart chemistry in polymeric nanomedicine. *Chem. Soc. Rev.* 43:6982–7012
12. Timko BP, Dvir T, Kohane DS. 2010. Remotely triggerable drug delivery systems. *Adv. Mater.* 22:4925–43
13. Tong R, Kohane DS. 2012. Shedding light on nanomedicine. *Wiley Interdiscip. Rev. Nanomed. Nanobiotechnol.* 4:638–62
14. Wong AD, DeWit MA, Gillies ER. 2012. Amplified release through the stimulus triggered degradation of self-immolative oligomers, dendrimers, and linear polymers. *Adv. Drug Deliv. Rev.* 64:1031–45
15. Amir RJ, Pessah N, Shamis M, Shabat D. 2003. Self-immolative dendrimers. *Angew. Chem. Int. Ed.* 42:4494–99
16. Sagi A, Weinstain R, Karton N, Shabat D. 2008. Self-immolative polymers. *J. Am. Chem. Soc.* 130:5434–35
17. de Gracia Lux C, Joshi-Barr S, Nguyen T, Mahmoud E, Schopf E, et al. 2012. Biocompatible polymeric nanoparticles degrade and release cargo in response to biologically relevant levels of hydrogen peroxide. *J. Am. Chem. Soc.* 134:15758–64
18. Weinstain R, Sagi A, Karton N, Shabat D. 2008. Self-immolative comb-polymers: multiple-release of side-reporters by a single stimulus event. *Chem. Eur. J.* 14:6857–61
19. Dewit MA, Gillies ER. 2009. A cascade biodegradable polymer based on alternating cyclization and elimination reactions. *J. Am. Chem. Soc.* 131:18327–34
20. Fan B, Trant JF, Wong AD, Gillies ER. 2014. Polyglyoxylates: a versatile class of triggerable self-immolative polymers from readily accessible monomers. *J. Am. Chem. Soc.* 136:10116–23
21. Fomina N, McFearin C, Sermsakdi M, Edigin O, Almutairi A. 2010. UV and near-IR triggered release from polymeric nanoparticles. *J. Am. Chem. Soc.* 132:9540–42
22. Paxton WF, Kistler KC, Olmeda CC, Sen A, St. Angelo SK, et al. 2004. Catalytic nanomotors: autonomous movement of striped nanorods. *J. Am. Chem. Soc.* 126:13424–31

23. Kagan D, Benchimol MJ, Claussen JC, Chuluun-Erdene E, Esener S, Wang J. 2012. Acoustic droplet vaporization and propulsion of perfluorocarbon-loaded microbullets for targeted tissue penetration and deformation. *Angew. Chem. Int. Ed.* 51:7519–22
24. Wang W, Li S, Mair L, Ahmed S, Huang TJ, Mallouk TE. 2014. Acoustic propulsion of nanorod motors inside living cells. *Angew. Chem. Int. Ed.* 53:3201–4
25. Garcia-Gradilla V, Orozco J, Sattayasamitsathit S, Soto F, Kuralay F, et al. 2013. Functionalized ultrasound-propelled magnetically guided nanomotors: toward practical biomedical applications. *ACS Nano* 7:9232–40
26. Gao W, Kagan D, Pak OS, Clawson C, Campuzano S, et al. 2012. Cargo-towing fuel-free magnetic nanoswimmers for targeted drug delivery. *Small* 8:460–67
27. Gao W, Sattayasamitsathit S, Manesh KM, Weihs D, Wang J. 2010. Magnetically powered flexible metal nanowire motors. *J. Am. Chem. Soc.* 132:14403–5
28. Ntziachristos V, Ripoll J, Weissleder R. 2002. Would near-infrared fluorescence signals propagate through large human organs for clinical studies? *Opt. Lett.* 27:333–35
29. Ntziachristos V, Ripoll J, Wang LV, Weissleder R. 2005. Looking and listening to light: the evolution of whole-body photonic imaging. *Nat. Biotechnol.* 23:313–20
30. Weissleder R. 2001. A clearer vision for in vivo imaging. *Nat. Biotechnol.* 19:316–17
31. Welsher K, Liu Z, Sherlock SP, Robinson JT, Chen Z, et al. 2009. A route to brightly fluorescent carbon nanotubes for near-infrared imaging in mice. *Nat. Nanotechnol.* 4:773–80
32. Srinivasan S, Pogue BW, Jiang S, Dehghani H, Kogel C, et al. 2003. Interpreting hemoglobin and water concentration, oxygen saturation, and scattering measured in vivo by near-infrared breast tomography. *PNAS* 100:12349–54
33. van Dam GM, Themelis G, Crane LMA, Harlaar NJ, Pleijhuis RG, et al. 2011. Intraoperative tumor-specific fluorescence imaging in ovarian cancer by folate receptor-α targeting: first in-human results. *Nat. Med.* 17:1315–19
34. Urano Y, Sakabe M, Kosaka N, Ogawa M, Mitsunaga M, et al. 2011. Rapid cancer detection by topically spraying a γ-glutamyltranspeptidase–activated fluorescent probe. *Sci. Transl. Med.* 3:110ra9
35. Weissleder R, Pittet MJ. 2008. Imaging in the era of molecular oncology. *Nature* 452:580–89
36. Hong G, Lee JC, Robinson JT, Raaz U, Xie L, et al. 2012. Multifunctional in vivo vascular imaging using near-infrared II fluorescence. *Nat. Med.* 18:1841–46
37. Ghosh D, Bagley AF, Na YJ, Birrer MJ, Bhatia SN, Belcher AM. 2014. Deep, noninvasive imaging and surgical guidance of submillimeter tumors using targeted M13-stabilized single-walled carbon nanotubes. *PNAS* 111:13948–53
38. Hong G, Robinson JT, Zhang Y, Diao S, Antaris AL, et al. 2012. In vivo fluorescence imaging with Ag_2S quantum dots in the second near-infrared region. *Angew. Chem. Int. Ed.* 51:9818–21
39. Ntziachristos V, Bremer C, Weissleder R. 2003. Fluorescence imaging with near-infrared light: new technological advances that enable in vivo molecular imaging. *Eur. Radiol.* 13:195–208
40. Sevick-Muraca EM, Houston JP, Gurfinkel M. 2002. Fluorescence-enhanced, near infrared diagnostic imaging with contrast agents. *Curr. Opin. Chem. Biol.* 6:642–50
41. Song CW. 1984. Effect of local hyperthermia on blood flow and microenvironment: a review. *Cancer Res.* 44:4721s–30s
42. Manzoor AA, Lindner LH, Landon CD, Park J-Y, Simnick AJ, et al. 2012. Overcoming limitations in nanoparticle drug delivery: triggered, intravascular release to improve drug penetration into tumors. *Cancer Res.* 72:5566–75
43. Zagar TM, Vujaskovic Z, Formenti S, Rugo H, Muggia F, et al. 2014. Two Phase I dose-escalation/pharmacokinetics studies of low temperature liposomal doxorubicin (LTLD) and mild local hyperthermia in heavily pretreated patients with local regionally recurrent breast cancer. *Int. J. Hyperthermia* 30:285–94
44. Hirsch LR, Stafford RJ, Bankson JA, Sershen SR, Rivera B, et al. 2003. Nanoshell-mediated near-infrared thermal therapy of tumors under magnetic resonance guidance. *PNAS* 100:13549–54
45. Huang X, Jain P, El-Sayed I, El-Sayed M. 2008. Plasmonic photothermal therapy (PPTT) using gold nanoparticles. *Lasers Med. Sci.* 23:217–28

46. Melancon MP, Zhou M, Li C. 2011. Cancer theranostics with near-infrared light-activatable multimodal nanoparticles. *Acc. Chem. Res.* 44:947–56
47. von Maltzahn G, Park J-H, Lin KY, Singh N, Schwöppe C, et al. 2011. Nanoparticles that communicate in vivo to amplify tumour targeting. *Nat. Mater.* 10:545–52
48. Park J-H, Gu L, von Maltzahn G, Ruoslahti E, Bhatia SN, Sailor MJ. 2009. Biodegradable luminescent porous silicon nanoparticles for in vivo applications. *Nat. Mater.* 8:331–36
49. Lovell JF, Jin CS, Huynh E, Jin H, Kim C, et al. 2011. Porphysome nanovesicles generated by porphyrin bilayers for use as multimodal biophotonic contrast agents. *Nat. Mater.* 10:324–32
50. Carter KA, Shao S, Hoopes MI, Luo D, Ahsan B, et al. 2014. Porphyrin–phospholipid liposomes permeabilized by near-infrared light. *Nat. Commun.* 5:3546
51. Yavuz MS, Cheng Y, Chen J, Cobley CM, Zhang Q, et al. 2009. Gold nanocages covered by smart polymers for controlled release with near-infrared light. *Nat. Mater.* 8:935–39
52. Tong R, Hemmati HD, Langer R, Kohane DS. 2012. Photoswitchable nanoparticles for triggered tissue penetration and drug delivery. *J. Am. Chem. Soc.* 134:8848–55
53. Tong R, Chiang HH, Kohane DS. 2013. Photoswitchable nanoparticles for in vivo cancer chemotherapy. *PNAS* 110:19048–53
54. Auzel F. 2003. Upconversion and anti-Stokes processes with f and d ions in solids. *Chem. Rev.* 104:139–74
55. Bloembergen N. 1959. Solid state infrared quantum counters. *Phys. Rev. Lett.* 2:84–85
56. Liu Q, Sun Y, Yang T, Feng W, Li C, Li F. 2011. Sub-10 nm hexagonal lanthanide-doped $NaLuF_4$ upconversion nanocrystals for sensitive bioimaging in vivo. *J. Am. Chem. Soc.* 133:17122–25
57. Wang F, Liu X. 2008. Upconversion multicolor fine-tuning: visible to near-infrared emission from lanthanide-doped $NaYF_4$ nanoparticles. *J. Am. Chem. Soc.* 130:5642–43
58. Wang F, Liu X. 2009. Recent advances in the chemistry of lanthanide-doped upconversion nanocrystals. *Chem. Soc. Rev.* 38(4):976–89
59. Wang Y-F, Liu G-Y, Sun L-D, Xiao J-W, Zhou J-C, Yan C-H. 2013. Nd^{3+}-sensitized upconversion nanophosphors: efficient in vivo bioimaging probes with minimized heating effect. *ACS Nano* 7:7200–6
60. Xie X, Gao N, Deng R, Sun Q, Xu Q-H, Liu X. 2013. Mechanistic investigation of photon upconversion in Nd^{3+}-sensitized core–shell nanoparticles. *J. Am. Chem. Soc.* 135:12608–11
61. Zou W, Visser C, Maduro JA, Pshenichnikov MS, Hummelen JC. 2012. Broadband dye-sensitized upconversion of near-infrared light. *Nat. Photon.* 6:560–64
62. Liu Q, Yin B, Yang T, Yang Y, Shen Z, et al. 2013. A general strategy for biocompatible, high-effective upconversion nanocapsules based on triplet–triplet annihilation. *J. Am. Chem. Soc.* 135:5029–37
63. Wang LV. 2009. Multiscale photoacoustic microscopy and computed tomography. *Nat. Photon* 3:503–9
64. Li M-L, Wang JC, Schwartz JA, Gill-Sharp KL, Stoica G, Wang LV. 2009. In-vivo photoacoustic microscopy of nanoshell extravasation from solid tumor vasculature. *J. Biomed. Opt.* 14:010507–3
65. Kim C, Cho EC, Chen J, Song KH, Au L, et al. 2010. In vivo molecular photoacoustic tomography of melanomas targeted by bioconjugated gold nanocages. *ACS Nano* 4:4559–64
66. Lu W, Melancon MP, Xiong C, Huang Q, Elliott A, et al. 2011. Effects of photoacoustic imaging and photothermal ablation therapy mediated by targeted hollow gold nanospheres in an orthotopic mouse xenograft model of glioma. *Cancer Res.* 71:6116–21
67. Kim J-W, Galanzha EI, Shashkov EV, Moon H-M, Zharov VP. 2009. Golden carbon nanotubes as multimodal photoacoustic and photothermal high-contrast molecular agents. *Nat. Nanotechnol.* 4:688–94
68. Kircher MF, de la Zerda A, Jokerst JV, Zavaleta CL, Kempen PJ, et al. 2012. A brain tumor molecular imaging strategy using a new triple-modality MRI-photoacoustic-Raman nanoparticle. *Nat. Med.* 18:829–34
69. Choi HS, Liu W, Liu F, Nasr K, Misra P, et al. 2010. Design considerations for tumour-targeted nanoparticles. *Nat. Nano* 5:42–47
70. Allen TM. 1988. Toxicity of drug carriers to the mononuclear phagocyte system. *Adv. Drug Deliv. Rev.* 2:55–67
71. Derfus AM, Chan WCW, Bhatia SN. 2004. Probing the cytotoxicity of semiconductor quantum dots. *Nano Lett.* 4:11–18

72. Hauck TS, Anderson RE, Fischer HC, Newbigging S, Chan WCW. 2010. In vivo quantum-dot toxicity assessment. *Small* 6:138–44
73. Balasubramanian SK, Jittiwat J, Manikandan J, Ong C-N, Yu LE, Ong W-Y. 2010. Biodistribution of gold nanoparticles and gene expression changes in the liver and spleen after intravenous administration in rats. *Biomaterials* 31:2034–42
74. Yang RH, Chang LW, Wu JP, Tsai MH, Wang HJ, et al. 2007. Persistent tissue kinetics and redistribution of nanoparticles, quantum dot 705, in mice: ICP-MS quantitative assessment. *Environ. Health Perspect.* 115:1339–43
75. Allen TM, Hansen C, Martin F, Redemann C, Yauyoung A. 1991. Liposomes containing synthetic lipid derivatives of poly(ethylene glycol) show prolonged circulation half-lives in vivo. *Biochim. Biophys. Acta* 1066:29–36
76. Allen TM. 1994. The use of glycolipids and hydrophilic polymers in avoiding rapid uptake of liposomes by the mononuclear phagocyte system. *Adv. Drug Deliv. Rev.* 13:285–309
77. Papahadjopoulos D, Allen TM, Gabizon A, Mayhew E, Matthay K, et al. 1991. Sterically stabilized liposomes: improvements in pharmacokinetics and antitumor therapeutic efficacy. *PNAS* 88:11460–64
78. Walkey CD, Olsen JB, Guo H, Emili A, Chan WCW. 2012. Nanoparticle size and surface chemistry determine serum protein adsorption and macrophage uptake. *J. Am. Chem. Soc.* 134:2139–47
79. Geng Y, Dalhaimer P, Cai SS, Tsai R, Tewari M, et al. 2007. Shape effects of filaments versus spherical particles in flow and drug delivery. *Nat. Nanotechnol.* 2:249–55
80. Oldenborg P-A, Zheleznyak A, Fang Y-F, Lagenaur CF, Gresham HD, Lindberg FP. 2000. Role of CD47 as a marker of self on red blood cells. *Science* 288:2051–54
81. Rodriguez PL, Harada T, Christian DA, Pantano DA, Tsai RK, Discher DE. 2013. Minimal "self" peptides that inhibit phagocytic clearance and enhance delivery of nanoparticles. *Science* 339:971–75
82. Perrault SD, Walkey C, Jennings T, Fischer HC, Chan WCW. 2009. Mediating tumor targeting efficiency of nanoparticles through design. *Nano Lett.* 9:1909–15
83. Jain RK. 1998. Delivery of molecular and cellular medicine to solid tumors. *J. Control. Release* 53:49–67
84. McKee TD, Grandi P, Mok W, Alexandrakis G, Insin N, et al. 2006. Degradation of fibrillar collagen in a human melanoma xenograft improves the efficacy of an oncolytic herpes simplex virus vector. *Cancer Res.* 66:2509–13
85. Netti PA, Berk DA, Swartz MA, Grodzinsky AJ, Jain RK. 2000. Role of extracellular matrix assembly in interstitial transport in solid tumors. *Cancer Res.* 60:2497–503
86. Yuan F, Leunig M, Huang SK, Berk DA, Papahadjopoulos D, Jain RK. 1994. Microvascular permeability and interstitial penetration of sterically stabilized (stealth) liposome in a human tumor xenograft. *Cancer Res.* 54:3352–56
87. Campbell RB, Fukumura D, Brown EB, Mazzola LM, Izumi Y, et al. 2002. Cationic charge determines the distribution of liposomes between the vascular and extravascular compartments of tumors. *Cancer Res.* 62:6831–36
88. Smith NR, Baker D, Farren M, Pommier A, Swann R, et al. 2013. Tumor stromal architecture can define the intrinsic tumor response to VEGF-targeted therapy. *Clin. Cancer Res.* 19:6943–56
89. Wong C, Stylianopoulos T, Cui JA, Martin J, Chauhan VP, et al. 2011. Multistage nanoparticle delivery system for deep penetration into tumor tissue. *PNAS* 108:2426–31
90. Cabral H, Matsumoto Y, Mizuno K, Chen Q, Murakami M, et al. 2011. Accumulation of sub-100 nm polymeric micelles in poorly permeable tumours depends on size. *Nat. Nanotechnol.* 6:815–23
91. Tang L, Yang X, Yin Q, Cai K, Wang H, et al. 2014. Investigating the optimal size of anticancer nanomedicine. *PNAS* 111:15344–49
92. Jensen SA, Day ES, Ko CH, Hurley LA, Luciano JP, et al. 2013. Spherical nucleic acid nanoparticle conjugates as an RNAi-based therapy for glioblastoma. *Sci. Transl. Med.* 5:209ra152
93. Jain RK. 2001. Normalizing tumor vasculature with anti-angiogenic therapy: a new paradigm for combination therapy. *Nat. Med.* 7:987–89
94. Chauhan VP, Stylianopoulos T, Martin JD, Popovic Z, Chen O, et al. 2012. Normalization of tumour blood vessels improves the delivery of nanomedicines in a size-dependent manner. *Nat. Nanotechnol.* 7:383–88

95. Mok W, Boucher Y, Jain RK. 2007. Matrix metalloproteinases-1 and -8 improve the distribution and efficacy of an oncolytic virus. *Cancer Res.* 67:10664–68
96. Provenzano PP, Cuevas C, Chang AE, Goel VK, Von Hoff DD, Hingorani SR. 2012. Enzymatic targeting of the stroma ablates physical barriers to treatment of pancreatic ductal adenocarcinoma. *Cancer Cell* 21:418–29
97. Feng S, Agoulnik IU, Bogatcheva NV, Kamat AA, Kwabi-Addo B, et al. 2007. Relaxin promotes prostate cancer progression. *Clin. Cancer Res.* 13:1695–702
98. Diop-Frimpong B, Chauhan VP, Krane S, Boucher Y, Jain RK. 2011. Losartan inhibits collagen I synthesis and improves the distribution and efficacy of nanotherapeutics in tumors. *PNAS* 108:2909–14
99. Chauhan VP, Martin JD, Liu H, Lacorre DA, Jain SR, et al. 2013. Angiotensin inhibition enhances drug delivery and potentiates chemotherapy by decompressing tumour blood vessels. *Nat. Commun.* 4:2516
100. Nakai Y, Isayama H, Ijichi H, Sasaki T, Takahara N, et al. 2013. A multicenter Phase II trial of gemcitabine and candesartan combination therapy in patients with advanced pancreatic cancer: GECA2. *Investig. New Drugs* 31:1294–99
101. Sugahara KN, Teesalu T, Karmali PP, Kotamraju VR, Agemy L, et al. 2010. Coadministration of a tumor-penetrating peptide enhances the efficacy of cancer drugs. *Science* 328:1031–35
102. Teesalu T, Sugahara KN, Kotamraju VR, Ruoslahti E. 2009. C-end rule peptides mediate neuropilin-1-dependent cell, vascular, and tissue penetration. *PNAS* 106:16157–62
103. Pang H-B, Braun GB, Friman T, Aza-Blanc P, Ruidiaz ME, et al. 2014. An endocytosis pathway initiated through neuropilin-1 and regulated by nutrient availability. *Nat. Commun.* 5:4904
104. Bertozzi CR. 2011. A decade of bioorthogonal chemistry. *Acc. Chem. Res.* 44:651–53
105. Jewett JC, Bertozzi CR. 2010. Cu-free click cycloaddition reactions in chemical biology. *Chem. Soc. Rev.* 39:1272–79
106. Devaraj NK, Weissleder R. 2011. Biomedical applications of tetrazine cycloadditions. *Acc. Chem. Res.* 44:816–27
107. Laughlin ST, Baskin JM, Amacher SL, Bertozzi CR. 2008. In vivo imaging of membrane-associated glycans in developing zebrafish. *Science* 320:664–67
108. Koo H, Lee S, Na JH, Kim SH, Hahn SK, et al. 2012. Bioorthogonal copper-free click chemistry in vivo for tumor-targeted delivery of nanoparticles. *Angew. Chem. Int. Ed.* 51:11836–40
109. Zlitni A, Janzen N, Foster FS, Valliant JF. 2014. Catching bubbles: targeting ultrasound microbubbles using bioorthogonal inverse-electron-demand Diels–Alder reactions. *Angew. Chem. Int. Ed.* 53:6459–63
110. Emmetiere F, Irwin C, Viola-Villegas NT, Longo V, Cheal SM, et al. 2013. ^{18}F-labeled-bioorthogonal liposomes for in vivo targeting. *Bioconjug. Chem.* 24:1784–89
111. Perrault SD, Chan WCW. 2010. In vivo assembly of nanoparticle components to improve targeted cancer imaging. *PNAS* 107:11194–99
112. Mellman I, Coukos G, Dranoff G. 2011. Cancer immunotherapy comes of age. *Nature* 480:480–89
113. Manolova V, Flace A, Bauer M, Schwarz K, Saudan P, Bachmann MF. 2008. Nanoparticles target distinct dendritic cell populations according to their size. *Eur. J. Immunol.* 38:1404–13
114. Reddy ST, van der Vlies AJ, Simeoni E, Angeli V, Randolph GJ, et al. 2007. Exploiting lymphatic transport and complement activation in nanoparticle vaccines. *Nat. Biotechnol.* 25:1159–64
115. Cho N-H, Cheong T-C, Min JH, Wu JH, Lee SJ, et al. 2011. A multifunctional core-shell nanoparticle for dendritic cell-based cancer immunotherapy. *Nat. Nanotechnol.* 6:675–82
116. de Titta A, Ballester M, Julier Z, Nembrini C, Jeanbart L, et al. 2013. Nanoparticle conjugation of CpG enhances adjuvancy for cellular immunity and memory recall at low dose. *PNAS* 110:19902–7
117. Nembrini C, Stano A, Dane KY, Ballester M, van der Vlies AJ, et al. 2011. Nanoparticle conjugation of antigen enhances cytotoxic T-cell responses in pulmonary vaccination. *PNAS* 108:E989–E97
118. Li AV, Moon JJ, Abraham W, Suh H, Elkhader J, et al. 2013. Generation of effector memory T cell–based mucosal and systemic immunity with pulmonary nanoparticle vaccination. *Sci. Transl. Med.* 5:204ra130
119. Rosenberg SA, Restifo NP, Yang JC, Morgan RA, Dudley ME. 2008. Adoptive cell transfer: a clinical path to effective cancer immunotherapy. *Nat. Rev. Cancer* 8:299–308

120. Stephan MT, Moon JJ, Um SH, Bershteyn A, Irvine DJ. 2010. Therapeutic cell engineering with surface-conjugated synthetic nanoparticles. *Nat. Med.* 16:1035–41
121. Weldon C, Tian B, Kohane DS. 2011. Nanotechnology for surgeons. *Wiley Interdiscip. Rev. Nanomed. Nanobiotechnol.* 3:223–28
122. Mehlen P, Puisieux A. 2006. Metastasis: a question of life or death. *Nat. Rev. Cancer* 6:449–58
123. Kohane DS, Langer R. 2010. Biocompatibility and drug delivery systems. *Chem. Sci.* 1:441–46